

LETTER TO THE EDITOR

Search for anions in molecular sources: C₄H⁻ detection in L1527^{*}

M. Agúndez¹, J. Cernicharo¹, M. Guélin², M. Gerin³, M. C. McCarthy⁴, and P. Thaddeus⁴

¹ Departamento de Astrofísica Molecular e Infrarroja, Instituto de Estructura de la Materia, CSIC, Serrano 121, 28006 Madrid, Spain
e-mail: [marce;cerni]@damir.iem.csic.es

² Institut de Radioastronomie Millimétrique, 300 rue de la Piscine, 38406 Saint Martin d'Hères, France
e-mail: guelin@iram.fr

³ LERMA, UMR 8112, CNRS, Observatoire de Paris and École Normale Supérieure, 24 rue l'Homond, 75231 Paris, France
e-mail: gerin@lra.ens.fr

⁴ Harvard-Smithsonian Center for Astrophysics, 60 Garden Street, Cambridge, MA 02138, USA
e-mail: [mccarthy;pthaddeus]@cfh.harvard.edu

Received 3 November 2007 / Accepted 28 November 2007

ABSTRACT

Aims. We present the results of a search for the negative ion C₄H⁻ in various dark clouds, low mass star-forming regions and photon-dominated regions (PDRs). We have also searched for C₆H⁻, C₂H⁻ and CN⁻ in some of the sources.

Methods. The millimeter-wave observations were carried out with the IRAM-30 m telescope.

Results. We detect C₄H⁻, through the $J = 9-8$ and $J = 10-9$ rotational transitions, in the low mass star-forming region L1527. We thus confirm the tentative detection of the $J = 9-8$ line recently reported toward this source. The [C₄H⁻]/[C₄H] ratio found is 0.011%, which is slightly lower than the value observed in IRC +10216, 0.024%, but above the 3 σ upper limit we derive in TMC-1, <0.0052%. We have also derived an upper limit for the [C₆H⁻]/[C₆H] ratio in the Horsehead Nebula, and for various anion-to-neutral ratios in the observed sources. These results are compared with recent chemical models.

Key words. astrochemistry – ISM: molecules – radio lines: ISM

1. Introduction

We have learnt that negatively charged molecules are present in the interstellar medium. Following the laboratory detection of the series of hydrocarbon anions C_{2n}H⁻ ($n = 1, 2, 3, 4$; McCarthy et al. 2006; Gupta et al. 2007; Brünken et al. 2007a) and of the smallest member of the isoelectronic series C_{2n+1}N⁻ ($n = 0$; Gottlieb et al. 2007), astronomical searches have succeeded in detecting the three largest anions of the first series in the C-rich envelope around the evolved star IRC +10216, C₆H⁻ and C₈H⁻ in the dark cloud TMC-1, and C₆H⁻ toward the low mass star-forming region L1527 (McCarthy et al. 2006; Cernicharo et al. 2007; Remijan et al. 2007; Brünken et al. 2007b; Sakai et al. 2007a). The smallest members of each series, C₂H⁻ and CN⁻, remain undetected in space.

It has been found that the abundance of the larger anions C₆H⁻ and C₈H⁻ represents a substantial fraction of that of their neutral counterparts (a few percent) while the smaller C₄H⁻ has an abundance much lower than C₄H (0.024% in IRC +10216). Thus, the anion-to-neutral ratio decreases when moving from large to small species. This trend was predicted many years ago by Herbst (1981), who discussed the formation and potential detectability of molecular anions in interstellar clouds. It was pointed out that the efficiency of electron radiative attachment greatly increases for species with a high electron affinity, such as the radicals C_{2n}H and C_{2n+1}N, and with a large number of vibrational states, i.e. a large size. Thus, the electron radiative attachment rate coefficients seems to be the crucial parameter controlling the anion-to-neutral ratio. Millar et al. (2007) have

calculated such rate coefficients and constructed chemical models which predict anions to be abundant in dark clouds and PDRs.

To explore how ubiquitous and abundant molecular anions are in the interstellar medium we have searched for C₄H⁻ with the IRAM-30 m telescope toward various dark clouds, low mass star-forming regions and PDRs. We have also searched for CN⁻, C₂H⁻ and C₆H⁻ in some of the sources. In this Letter we present the results of these searches, which have led to the positive detection of C₄H⁻ in the low mass star-forming region L1527.

2. Observations

The observations were carried out with the IRAM-30 m telescope from 24th July to 2nd August 2007. We searched for molecular anions in the starless cores: TMC-1 (at the cyanopolyne peak), Barnard 1 (at the B1-b core) and L134N; and in the low mass star-forming regions L1527 and L483, at the position of their embedded IRAS sources. In PDRs, molecular anions are predicted to have a peak abundance in the low extinction, $A_V \sim 1.5-3$, interface where the transition of C⁺ to CO occurs (Millar et al. 2007). We thus searched for anions toward such positions in three PDRs: the Horsehead Nebula at the so-called IR peak where the greatest hydrocarbon emission is observed (Teyssier et al. 2004; Pety et al. 2005), the Orion Bar at the (CO) position where CF⁺ was discovered (Neufeld et al. 2006), and the reflection nebula NGC 7023 at the so-called PDR peak where CO⁺ has been observed (Fuente & Martín-Pintado 1997).

We used SIS receivers operating at 3 mm and 1 mm in single-sideband mode with image rejections >20 dB at 3 mm and ≥ 10 dB at 1 mm. System temperatures were 100–140 K

^{*} Based on observations carried out with the IRAM 30 m telescope. IRAM is supported by INSU/CNRS (France), MPG (Germany) and IGN (Spain).

Table 1. Observed line parameters.

Source	Molecule	Transition	Frequency (MHz)	T_A^* (mK)	$\Delta\nu$ (km s ⁻¹)	V_{LSR} (km s ⁻¹)	$\int T_A^* d\nu$ (mK km s ⁻¹)	η_b^c
TMC-1 ^e	C ₄ H	$N = 9-8$ $J = 9.5-8.5^d$	85 634.012	678(12)	0.58(8)	+5.83(4)	417(11)	0.82
	C ₄ H	$N = 9-8$ $J = 8.5-7.5^d$	85 672.578	626(11)	0.58(8)	+5.74(4)	386(10)	0.82
	C ₄ H ⁻	$J = 9-8$	83 787.263	1.5 ^a	–	–	2.8 ^b	0.82
	CN ⁻	$J = 2-1$	224 525.061	7.8 ^a	–	–	14.5 ^b	0.59
	C ₂ H ⁻	$J = 3-2$	249 824.940	3.5 ^a	–	–	6.6 ^b	0.53
Barnard 1 ^e	C ₄ H	$N = 9-8$ $J = 9.5-8.5^d$	85 634.012	145(9)	1.21(7)	+6.79(5)	186(8)	0.82
	C ₄ H	$N = 9-8$ $J = 8.5-7.5^d$	85 672.578	133(8)	1.09(7)	+6.64(5)	154(7)	0.82
	C ₄ H ⁻	$J = 9-8$	83 787.263	1.2 ^a	–	–	4.4 ^b	0.82
	CN ⁻	$J = 2-1$	224 525.061	2.8 ^a	–	–	10.3 ^b	0.59
	C ₂ H ⁻	$J = 3-2$	249 824.940	7.9 ^a	–	–	29 ^b	0.53
L134N	C ₄ H	$N = 9-8$ $J = 9.5-8.5$	85 634.012	131(7)	0.33(4)	+2.47(4)	46(5)	0.82
	C ₄ H	$N = 9-8$ $J = 8.5-7.5$	85 672.578	122(6)	0.29(4)	+2.38(4)	38(4)	0.82
	C ₄ H ⁻	$J = 9-8$	83 787.263	2.9 ^a	–	–	2.9 ^b	0.82
	CN ⁻	$J = 2-1$	224 525.061	14 ^a	–	–	14 ^b	0.59
L1527 ^e	C ₄ H ⁻	$J = 9-8$	83 787.263	13(2)	0.62(9)	+5.80(3)	8(1)	0.82
	C ₄ H ⁻	$J = 10-9$	93 096.551	11(2)	0.59(9)	+5.90(4)	7(1)	0.81
	C ₄ H	$N = 9-8$ $J = 9.5-8.5^d$	85 634.012	947(11)	0.74(6)	+5.95(2)	747(11)	0.82
	C ₄ H	$N = 9-8$ $J = 8.5-7.5^d$	85 672.578	871(11)	0.77(6)	+5.89(2)	712(11)	0.82
	C ₄ H	$N = 11-10$ $J = 11.5-10.5^d$	104 666.566	681(10)	0.75(6)	+5.92(2)	542(10)	0.79
	C ₄ H	$N = 11-10$ $J = 10.5-9-5^d$	104 705.109	656(10)	0.70(6)	+5.88(2)	487(10)	0.79
	C ₄ H	$N = 12-11$ $J = 12.5-11.5$	114 182.516	712(14)	0.61(4)	+5.93(3)	462(13)	0.78
	C ₄ H	$N = 12-11$ $J = 11.5-10.5$	114 221.039	663(13)	0.58(4)	+5.85(3)	406(12)	0.78
	CN ⁻	$J = 2-1$	224 525.061	2.3 ^a	–	–	5.5 ^b	0.59
	C ₂ H ⁻	$J = 3-2$	249 824.940	3.5 ^a	–	–	6.7 ^b	0.53
L483 ^e	C ₄ H	$N = 9-8$ $J = 9.5-8.5^d$	85 634.012	387(15)	0.60(6)	+5.27(4)	249(12)	0.82
	C ₄ H	$N = 9-8$ $J = 8.5-7.5^d$	85 672.578	332(15)	0.70(6)	+5.33(4)	249(12)	0.82
	C ₄ H ⁻	$J = 9-8$	83 787.263	4.5 ^a	–	–	9.3 ^b	0.82
	CN ⁻	$J = 2-1$	224 525.061	11.5 ^a	–	–	28 ^b	0.59
Horsehead ^d	C ₄ H	$N = 9-8$ $J = 9.5-8.5^d$	85 634.012	199(10)	0.86(8)	+10.72(4)	181(9)	0.82
	C ₄ H	$N = 9-8$ $J = 8.5-7.5^d$	85 672.578	155(8)	0.81(8)	+10.69(4)	133(9)	0.82
	C ₆ H	$^2\Pi_{3/2}$ $J = 29.5-28.5$ f ^d	81 777.898	13(2)	0.93(16)	+10.76(8)	13(2)	0.82
	C ₆ H	$^2\Pi_{3/2}$ $J = 29.5-28.5$ e ^d	81 801.254	10(2)	0.97(21)	+10.81(9)	11(2)	0.82
	C ₄ H ⁻	$J = 9-8$	83 787.263	1.9 ^a	–	–	5.0 ^b	0.82
	C ₆ H ⁻	$J = 30-29$	82 608.285	1.5 ^a	–	–	4.6 ^b	0.82
	CN ⁻	$J = 2-1$	224 525.061	2.2 ^a	–	–	4.9 ^b	0.59
Orion Bar ^e	C ₄ H	$N = 9-8$ $J = 9.5-8.5^d$	85 634.012	58(5)	1.86(11)	+10.77(6)	116(7)	0.82
	C ₄ H	$N = 9-8$ $J = 8.5-7.5^d$	85 672.578	55(10)	2.54(13)	+10.60(9)	149(8)	0.82
	C ₄ H ⁻	$J = 9-8$	83 787.263	1.2 ^a	–	–	8.4 ^b	0.82
	CN ⁻	$J = 2-1$	224 525.061	3.2 ^a	–	–	18 ^b	0.59
NGC 7023 ^{e,f}	CN ⁻	$J = 2-1$	224 525.061	6.4 ^a	–	–	16.4 ^b	0.59
	C ₂ H ⁻	$J = 3-2$	249 824.940	9.5 ^a	–	–	20 ^b	0.53

NOTE. The line parameters have been obtained from Gaussian fits. Number in parentheses are 1σ uncertainties in units of the last digits. The observed positions are: TMC-1 $\alpha_{2000.0} = 04^{\text{h}}41^{\text{m}}41.9^{\text{s}}$, $\delta_{2000.0} = +25^{\circ}41'27.0''$; Barnard 1 $\alpha_{2000.0} = 03^{\text{h}}33^{\text{m}}20.8^{\text{s}}$, $\delta_{2000.0} = +31^{\circ}07'34.0''$; L134N $\alpha_{2000.0} = 15^{\text{h}}54^{\text{m}}06.6^{\text{s}}$, $\delta_{2000.0} = -02^{\circ}52'19.1''$; L1527 $\alpha_{2000.0} = 04^{\text{h}}39^{\text{m}}53.9^{\text{s}}$, $\delta_{2000.0} = +26^{\circ}03'11.0''$; L483 $\alpha_{2000.0} = 18^{\text{h}}17^{\text{m}}29.8^{\text{s}}$, $\delta_{2000.0} = -04^{\circ}39'38.3''$; Horsehead $\alpha_{2000.0} = 05^{\text{h}}40^{\text{m}}53.7^{\text{s}}$, $\delta_{2000.0} = -02^{\circ}28'04.0''$; Orion Bar $\alpha_{2000.0} = 05^{\text{h}}35^{\text{m}}22.8^{\text{s}}$, $\delta_{2000.0} = -05^{\circ}25'01.0''$; and NGC 7023 $\alpha_{2000.0} = 21^{\text{h}}01^{\text{m}}32.6^{\text{s}}$, $\delta_{2000.0} = +68^{\circ}10'27.0''$.

^a rms noise averaged over the line width. ^b 3σ upper limit assuming the same line width as the neutral. ^c η_b is $B_{\text{eff}}/F_{\text{eff}}$, i.e. the ratio of T_A^* to T_{mb} .

^d Line observed with a spectral resolution of 80 kHz. ^e The $N = 2-1$ $J = 5/2-3/2$ transition of CN at 226.8 GHz was observed in this source with a S/N ratio higher than 6; line widths are 0.58 km s⁻¹ in TMC-1, 1.15 km s⁻¹ in Barnard 1, 0.75 km s⁻¹ in L1527, 0.76 km s⁻¹ in L483, 0.70 km s⁻¹ in the Horsehead, 1.76 km s⁻¹ in the Orion Bar, and 0.80 km s⁻¹ in NGC 7023. ^f The $N = 3-2$ transition of C₂H at 262.0 GHz was observed in NGC 7023 with a S/N ratio higher than 20 and a line width of 0.65 km s⁻¹.

at 3 mm and 300–500 K at 1 mm. An autocorrelator was used as the back end. The spectral resolution at 3 mm was 40 kHz (~ 0.13 km s⁻¹), except for some observations of neutral species for which 80 kHz was used (see Table 1), and 80 kHz at 1 mm (~ 0.10 km s⁻¹). We used the frequency switching technique with a frequency throw of 7.14 MHz. Pointing and focus were checked every 1–2 h observing nearby planets or quasars. The list of observed molecules and transitions is given in Table 1.

3. Results and discussion

Most of the observing time was dedicated to the search for C₄H⁻ in TMC-1 and L1527, and for C₆H⁻ in the Horsehead Nebula. We could only detect C₄H⁻ in L1527 through the $J = 9-8$ and $J = 10-9$ rotational lines (shown in Fig. 1 at a spectral resolution of 40 kHz) which are observed with a signal-to-noise ratio in T_A^* of 6 and 5 respectively. We thus confirm the tentative detection

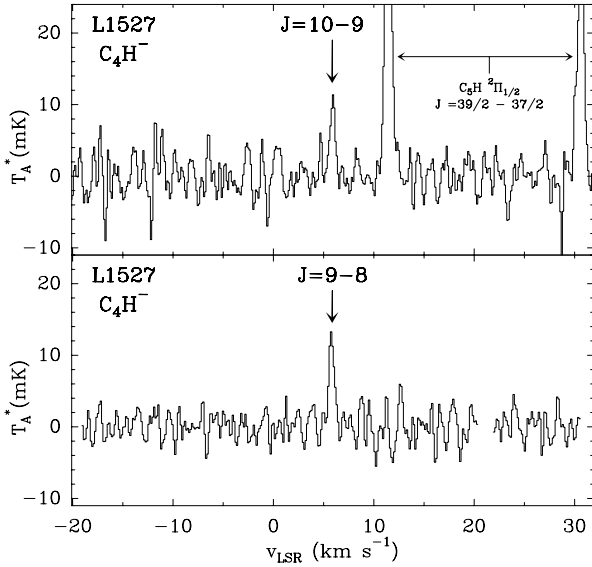


Fig. 1. $J = 9-8$ and $J = 10-9$ transitions of C_4H^- observed toward L1527 in 13.8 h and 22.1 h of integration time respectively.

of the $J = 9-8$ line announced by Sakai et al. (2007a). The lines have a Gaussian-like profile with a width of 0.6 km s^{-1} and are centered at a source velocity of $+5.85 \text{ km s}^{-1}$. Similar line properties are also found for C_4H (see Table 1), for C_6H and C_6H^- (Sakai et al. 2007a), and for other carbon chains observed in L1527 (Sakai et al. 2007b). The rms noise levels reached in the other searches for anions, a few mK in T_A^* in most of the cases, are given in Table 1.

We have calculated beam averaged column densities (see Table 2) under the LTE approximation. In L1527, the column density of C_4H^- is $1.6 \times 10^{10} \text{ cm}^{-2}$ and that of C_4H is $1.5 \times 10^{14} \text{ cm}^{-2}$. The rotational temperature (T_{rot}) obtained for C_4H is $14.1 \pm 1.6 \text{ K}$, while in the case of C_4H^- the two observed lines suggests a value of 14 K which is in agreement with that found for C_4H . In the rest of the cases T_{rot} has been fixed: for the dense cores L1527 and L483 we assumed that T_{rot} is equal to the gas kinetic temperature, 14 K and 10 K respectively (Sakai et al. 2007b; Tafalla et al. 2000), and adopted $T_{\text{rot}} = 5 \text{ K}$ for the cold dark clouds and $T_{\text{rot}} = 15 \text{ K}$ for the PDRs.

The anion-to-neutral ratios derived in various sources from this and previous works are given in Table 3. In the C_nH^- series, the ratios (or limits to ratios) observed for C_6H^- and C_8H^- are always above 1%. They are about two orders of magnitude lower for C_4H^- and even smaller for C_2H^- (at least in IRC +10216). In the case of the $[CN^-]/[CN]$ ratio, the lowest upper limits derived (0.2% for the lowest) are less constraining than in the case of C_2H^- .

The anion-to-neutral ratio maybe expressed in terms of the processes of formation and destruction of the anion. In steady state we have (see Cernicharo et al. 2007):

$$\frac{[A^-]}{[A]} = \frac{k_{\text{ea}}[e^-]}{k_{B^+}[B^+] + k_{N^0}[N^0] + \Gamma_{\text{ph}}/n} \quad (1)$$

where n is the gas volume density and it is assumed that the anion A^- forms by attachment of an electron e^- on A (with a rate constant k_{ea}) and can be destroyed by reactions with cations B^+ (k_{B^+}), neutral atoms N^0 (k_{N^0}), and by photodetachment (Γ_{ph}). Carbon chain anions are known to react rapidly with H and O atoms, and somewhat more slowly with N atoms (Eichelberger et al. 2007). Assuming rather standard rate constants for the other destruction processes ($k_{B^+} = 10^{-7} \text{ cm}^3 \text{ s}^{-1}$

Table 2. Column densities.

Source	Molecule	$T_{\text{rot}}(\text{K})$	$N(10^{10} \text{ cm}^{-2})$
TMC-1	C_4H^- (C_4H)	5.0 ^a (5.0 ^a)	<3.7 ^b (71 000)
	CN^- (CN)	5.0 ^a (5.0 ^a)	<140 ^b (4700)
	C_2H^-	5.0 ^a	<22 ^b
Barnard 1	C_4H^- (C_4H)	5.0 ^a (5.0 ^a)	<6 ^b (25 000)
	CN^- (CN)	5.0 ^a (5.0 ^a)	<84 ^b (21 000)
	C_2H^-	5.0 ^a	<15 ^b
L134N	C_4H^- (C_4H)	5.0 ^a (5.0 ^a)	<3.8 ^b (6100)
	CN^-	5.0 ^a	<130 ^b
L1527	C_4H^- (C_4H)	13.6 (14.1)	1.6 (15 000)
	CN^- (CN)	14.0 ^a (14.0 ^a)	<9.8 ^b (>4800)
	C_2H^-	14.0 ^a	<1.8 ^b
L483	C_4H^- (C_4H)	10.0 ^a (10.0 ^a)	<2.3 ^b (6900)
	CN^- (CN)	10.0 ^a (10.0 ^a)	<90 ^b (>7100)
Horsehead	C_4H^- (C_4H)	15.0 ^a (15.0 ^a)	<1.0 ^b (3000)
	C_6H^- (C_6H)	15.0 ^a (15.0 ^a)	<8.0 ^b (90)
	CN^- (CN)	15.0 ^a (15.0 ^a)	<12 ^b (2200)
Orion Bar	C_4H^- (C_4H)	15.0 ^a (15.0 ^a)	<1.6 ^b (2500)
	CN^- (CN)	15.0 ^a (15.0 ^a)	<46 ^b (27 000)
NGC 7023	CN^- (CN)	15.0 ^a (15.0 ^a)	<37 ^b (1400)
	C_2H^- (C_2H)	15.0 ^a (15.0 ^a)	<3.1 ^b (8900)

NOTE. Parameters for the neutral species are given in parentheses. $\mu(C_2H^-) = 3.1 \text{ D}$; $\mu(C_4H^-) = 6.2 \text{ D}$; $\mu(C_6H^-) = 8.2 \text{ D}$; $\mu(CN^-) = 0.65 \text{ D}$. ^a Assumed rotational temperature. ^b 3σ upper limit.

and Γ_{ph} from Millar et al. 2007), we may use the observed $[A^-]/[A]$ ratio to derive the relevant electron attachment rate constant $k_{\text{ea}}(A)$. This approach was used by Cernicharo et al. (2007) in the context of a chemical model of IRC +10216 to derive $k_{\text{ea}}(C_4H)$ and $k_{\text{ea}}(C_6H)$. Here we have revised that model, including loss of anions by reaction with atoms other than H, to arrive at:

$$\begin{aligned} k_{\text{ea}}(C_8H) &= 2.5 \times 10^{-8} (T/300)^{-1/2} \text{ cm}^3 \text{ s}^{-1} \\ k_{\text{ea}}(C_6H) &= 1.4 \times 10^{-8} (T/300)^{-1/2} \text{ cm}^3 \text{ s}^{-1} \\ k_{\text{ea}}(C_4H) &= 9 \times 10^{-11} (T/300)^{-1/2} \text{ cm}^3 \text{ s}^{-1} \\ k_{\text{ea}}(C_2H) &< 1.5 \times 10^{-11} (T/300)^{-1/2} \text{ cm}^3 \text{ s}^{-1}. \end{aligned} \quad (2)$$

The values of $k_{\text{ea}}(C_4H)$ and $k_{\text{ea}}(C_6H)$ at temperatures of 10–30 K are similar to those derived in Cernicharo et al. (2007). There exists a clear correlation between the value of k_{ea} and the observed anion-to-neutral ratio, which simply indicates that the latter is mostly controlled by the electron attachment reaction, the destruction processes being assumed similar for all anions. The rate constants k_{ea} obtained for C_6H and C_3H are of the same order of magnitude as the theoretical values reported by Millar et al. (2007), although the value for C_4H is more than one order of magnitude lower than the theoretical one. In fact, the chemical models of Millar et al. (2007) systematically overestimate the anion-to-neutral ratio for C_4H^- . They calculate values of the $[C_4H^-]/[C_4H]$ ratio in IRC +10216, in TMC-1 (at early time) and in the Horsehead Nebula of 0.77%, 0.13% and 3.5% respectively, which are higher by a factor of 20–100 than the values derived from observations (see Table 3). It seems that the theory of electron radiative attachment (Terzieva & Herbst 2000) fails for small molecules (the much lower dipole moment of C_4H compared to C_6H and C_8H could play a role in diminishing the efficiency for electron attachment; see Brünken et al. 2007b), or that there are important destruction processes for small anions so far not considered (e.g. reaction with neutral molecules).

Table 3. Anion-to-neutral ratios (in %) in various molecular sources.

	IRC +10216	TMC-1	Barnard 1	L134N	L1527	L483	Horsehead	Orion Bar	NGC 7023
$[C_2H^-]/[C_2H]$	<0.0030 ^(1,2)	<0.033 ^(6,7)	<0.048 ^(6,7)	<0.25 ^(9,10)	<0.0036 ^(6,7)				<0.035 ⁽⁶⁾
$[C_4H^-]/[C_4H]$	0.024 ⁽³⁾	<0.0052 ⁽⁶⁾	<0.024 ⁽⁶⁾	<0.062 ⁽⁶⁾	0.011 ⁽⁶⁾	<0.033 ⁽⁶⁾	<0.033 ⁽⁶⁾	<0.064 ⁽⁶⁾	
$[C_6H^-]/[C_6H]$	6.2–8.6 ^(3,4)	1.6 ⁽⁸⁾			9.3 ⁽¹¹⁾		<8.9 ⁽⁶⁾		
$[C_8H^-]/[C_8H]$	26 ⁽⁵⁾	4.6 ⁽⁸⁾							
$[CN^-]/[CN]$	<0.52 ⁽¹⁾	<1.9 ⁽⁶⁾	<0.40 ⁽⁶⁾	<6.5 ^(6,10)	<0.20 ⁽⁶⁾	<1.3 ⁽⁶⁾	<0.55 ⁽⁶⁾	<0.17 ⁽⁶⁾	<2.6 ⁽⁶⁾

REFERENCES. (1) Unpublished IRAM-30 m data; (2) Cernicharo et al. (2000); (3) Cernicharo et al. (2007); (4) Kasai et al. (2007); (5) Remijan et al. (2007); (6) This work; (7) Sakai et al. (2007b); (8) Brünken et al. (2007b); (9) Morisawa et al. (2005); (10) Dickens et al. (2000); (11) Sakai et al. (2007a).

The presence of molecular anions seems to be favored in IRC +10216, where three different anions have been observed with relatively high anion-to-neutral ratios, compared to the other sources. The ratios are in particular larger in IRC +10216 than in TMC-1, most probably due to a larger ionization degree in the former.

Comparing the dense cores TMC-1 and L1527, we note that molecular anions are present at a higher level in the latter, as indicated by the larger $[C_6H^-]/[C_6H]$ and $[C_4H^-]/[C_4H]$ ratios. This has been interpreted by Sakai et al. (2007a) as due to a higher gas density in L1527 ($\sim 10^6$ cm⁻³; Sakai et al. 2007b) compared to that in TMC-1 (10^4 cm⁻³). An increase in the gas density makes the abundance of H atoms decrease more than that of electrons¹. Thus according to Eq. (1) (the term Γ_{ph}/n drops for a dense cloud shielded from UV photons,) this results in an increase of the anion-to-neutral-ratio which approaches its maximum value k_{ea}/k_{B^+} , achieved in the limit when reactions with cations dominate the destruction of anions, i.e. $k_{B^+}[B^+] \gg k_{N^0}[N^0]$ and assuming $[B^+] = [e^-]$.

An interesting difference between TMC-1 and L1527 is that the former is a starless quiescent core while the latter harbors an embedded protostar (IRAS 04368+2557) with an associated bipolar outflow and an infalling envelope of about 30'' (Ohashi et al. 1997). The outflow is revealed in the high velocity (~ 3 km s⁻¹) wings of some molecular lines such as HCO⁺ $J = 1-0$ (Sakai et al. 2007b). These wings are not present in the C₄H⁻ lines, which rules out the presence of a substantial fraction of anion molecules in the outflow. The gravitational infall is indicated by the two-peak asymmetry, with a brighter blue peak, in the profiles of some optically thick lines of c-C₃H₂ and H₂CO (Myers et al. 1995). Such a profile is not visible in any of the C₄H and C₄H⁻ lines observed in L1527, although they are optically thin. Small mapping observations of the $N = 9-8$ transition indicates that C₄H has an extended distribution ($\sim 40''$) in all directions around the protostar and that the line width increases when approaching to the central position (Sakai et al. 2007b). This latter signature was also observed by Myers et al. (1995) in the c-C₃H₂ $2_{1,2}-1_{0,1}$ line and was interpreted as due to infall motion. Unfortunately, the rather weak C₄H⁻ lines observed in L1527 leave little chance to map their emission.

In the PDRs, the upper limits on the anion-to-neutral ratios are not as low as in the rest of the sources due to the lower abundance of carbon chains. Nevertheless, we find values much lower than those predicted by chemical models. In particular, Millar et al. (2007) overestimate by more than a factor of 100 the anion-to-neutral ratio for C₄H⁻ in the Horsehead Nebula. The discrepancy could lie in the value of $k_{ea}(C_4H)$ used in the models, which is probably too large. In the case of C₆H⁻, the predicted

ratio (470%) is larger than our upper limit by a factor of 50. The fact that chemical models reproduce much better the observed $[C_6H^-]/[C_6H]$ ratio in IRC +10216 and TMC-1 (within a factor of 4) than in the Horsehead Nebula suggests that in PDRs the global destruction rate of the anion could be underestimated.

This study has shown that molecular anions, despite the weakness of their millimeter emission, may be used to probe the chemical and physical conditions of interstellar clouds (see also Flower et al. 2007). Further laboratory and theoretical work are necessary for a more complete interpretation of the astronomical observations.

Sakai et al. (2007c) report the tentative detection of the C₄H⁻ $J = 9-8$ line in L1527. They derive a column density of 1.1×10^{10} cm⁻² which is in good agreement with the value obtained by us.

Acknowledgements. We would like to thank the IRAM staff and the 30 m telescope operators for their assistance during the observations and N. Marcelino for useful advices on the frequency switching observing mode. We also thank the anonymous referee for helpful suggestions. We acknowledge N. Sakai, T. Sakai and S. Yamamoto for communicating their observational results prior to publication. This work has been supported by Spanish MEC trough grants AYA2003-2785, AYA2006-14876 and ESP2004-665 and by Spanish CAM under PRICIT project S-0505/ESP-0237 (ASTROCAM). MA also acknowledges grant AP2003-4619 from Spanish MEC.

References

- Brünken, S., Gottlieb, C. A., Gupta, H., et al. 2007a, A&A, 464, L33
 Brünken, S., Gupta, H., Gottlieb, C. A., et al. 2007b, ApJ, 664, L43
 Cernicharo, J., Guélin, M., & Kahane, C. 2000, A&AS, 142, 181
 Cernicharo, J., Guélin, M., Agúndez, M., et al. 2007, A&A, 467, L37
 Dickens, J. E., Irvine, W. M., Snell, R. L., et al. ApJ, 542, 870
 Eichelberger, B., Snow, T. P., Barckholtz, C., & Bierbaum, V. M. 2007, ApJ, 667, 1283
 Flower, D. R., Pineau des Forêts, G., & Walmsley, C. M. 2007, A&A, 474, 923
 Fuente, A., & Martín-Pintado, J. 1997, ApJ, 477, L107
 Gottlieb, C. A., Brünken, S., McCarthy, M. C., & Thaddeus, P. 2007, J. Chem. Phys., 126, 191101
 Gupta, H., Brünken, S., Tamassia, F., et al. 2007, ApJ, 655, L57
 Herbst, E. 1981, Nature, 289, 656
 Kasai, Y., Kagi, E., & Kawaguchi, K. 2007, ApJ, 661, L61
 McCarthy, M. C., Gottlieb, C. A., Gupta, H., & Thaddeus, P. 2006, ApJ, 652, L141
 Millar, T. J., Walsh, C., Cordiner, M. A., et al. 2007, ApJ, 662, L87
 Morisawa, Y., Hoshina, H., Kato, Y., et al. 2005, PASJ, 57, 325
 Myers, P. C., Bachiller, R., Caselli, P., et al. 1995, ApJ, 449, L65
 Neufeld, D. A., Schilke, P., Menten, K. M., et al. 2006, A&A, 454, L37
 Ohashi, N., Hayashi, M., Ho, P. T. P., & Momose, M. 1997, ApJ, 475, 211
 Pety, J., Teyssier, D., Fossé, D., et al. 2005, A&A, 435, 885
 Remijan, A. J., Hollis, J. M., Lovas, F. J., et al. 2007, ApJ, 664, L47
 Sakai, N., Sakai, T., Osamura, Y., & Yamamoto, S. 2007a, ApJ, 667, L65
 Sakai, N., Sakai, T., Hirota, T., & Yamamoto, S. 2007b, ApJ, preprint doi:10.1086/523635
 Sakai, N., Sakai, T., & Yamamoto, S. 2007c, ApJ, in press
 Tafalla, M., Myers, P. C., Mardones, D., & Bachiller, R. 2000, A&A, 359, 967
 Terzieva, R., & Herbst, E. 2000, Int. J. Mass Spectr., 201, 135
 Teyssier, D., Fossé, D., Gerin, M., et al. 2004, A&A, 417, 135

¹ It is predicted that in a dense cloud the abundance of H atoms varies with the gas density as the inverse while that of electrons varies only as the inverse of the square root (see e.g. Flower et al. 2007).